Cardiovasc Intervent Radiol (2008) 31:1184–1192
DOI 10.1007/s00270-008-9392-7

LABORATORY INVESTIGATION

Reduction of Late In-Stent Stenosis in a Porcine Coronary Artery Model by Cobalt Chromium Stents with a Nanocoat of Polyphosphazene (Polyzene-F)

Ulrike Stampfl · Christof-Matthias Sommer · Heidi Thierjung · Sibylle Stampfl · Ruben Lopez-Benitez · Boris Radeleff · Irina Berger · Goetz M. Richter

Received: 1 April 2008 / Accepted: 25 June 2008 / Published online: 13 August 2008

Abstract The purpose of this study was to investigate the potential of nanoscale coating with the highly biocompatible polymer Polyzene-F (PZF), in combination with cobalt chromium and stainless steel stents, to reduce in-stent stenosis, thrombogenicity, and vessel wall injury and inflammation. One bare cobalt chromium, PZF-nanocoated stainless steel or PZF-nanocoated cobalt chromium stent was implanted in right coronary artery of 30 mini-pigs (4- or 12-week follow-up). Primary study end points were in-stent stenosis and thrombogenicity. Secondary study end points were vessel wall injury and inflammation as evaluated by microscopy and a new immunoreactivity score applying C-reactive protein (CRP), tumor-necrosis factor alpha (TNFα), and TGFβ. At 12 weeks, angiography showed a significantly lower average loss in lumen diameter (2.1% ± 3.05%) in PZF-nanocoated cobalt chromium stents compared with stents in the other groups (9.73% ± 4.93% for bare cobalt chromium stents and 9.71% ± 7% for PZF-nanocoated stainless steel stents; $p = 0.04$), which was confirmed at microscopy (neointima 40.7 ± 16 μm in PZF-nanocoated cobalt chromium stents, 74.7 ± 57.6 μm in bare cobalt chromium stents, and 141.5 ± 109 μm in PZF-nanocoated stainless steel stents; $p = 0.04$). Injury and inflammation scores were low in all stents and were without significant differences. PZF-nanocoated cobalt chromium stents provided the highest efficacy in reducing in-stent stenosis at long-term follow-up. The PZF nanocoat proved to be biocompatible with respect to thromboresistance and inflammation. Our data suggest that its combination with cobalt chromium stents might provide an interesting passive stent platform.

Keywords In-stent stenosis · Cobalt chromium · Polymer coating · Polyzene®-F · Inflammation

U. Stampfl · C.-M. Sommer · H. Thierjung · S. Stampfl · R. Lopez-Benitez · B. Radeleff · G. M. Richter (✉)
Department of Radiology, University of Heidelberg, INF 110, 69120 Heidelberg, Germany
e-mail: goetz_richter@med.uni-heidelberg.de

I. Berger
Department of Pathology, University of Heidelberg, INF 110, 69120 Heidelberg, Germany

Introduction

In-stent stenosis caused by neointimal proliferation remains a limiting factor for long-term success after coronary artery stenting [1]. In previous studies, a variety of stent parameters such as strut thickness, geometric arrangement, backbone material, stent coating and, more recently, elution of biologically active drugs from the strut surface have been identified to influence long-term outcome [2–5].

Recently, several polymers have been investigated to serve as permanent stent coating and to improve thromboresistance and in-stent stenosis [6–8]. In this context, the polymer PZF (poly(bis(trifluoroethoxy)phosphazene), which has a $[P = N]_n$ backbone and trifluoroethanol side groups and is marketed as Polyzene-F (Celonova Biosciences, Newnan, GA), showed promising results with low neointimal proliferation and antithrombotic surface properties [9, 10]. In a recent study of our group in a mini-pig iliac and renal artery model, only very mild vessel wall inflammation was found, demonstrating excellent biocompatibility of the PZF coating [11]. In a porcine coronary artery study performed by Huang, no significant differences between PTFEP (earlier version of poly(bis(trifluoroethoxy)phosphazene)-coated and bare stainless steel stents were detected with respect to vessel

wall inflammation and restenosis [10]. Recently, it was demonstrated that none of the PZF-coated stainless steel stents and 30% of the uncoated controls showed binary stenosis at long-term follow-up in a porcine coronary artery model [12]. Furthermore, only mild vessel wall inflammation, without significant differences between uncoated and PZF-coated stents, was found.

In the study described here, we investigated whether these results could be corroborated or even improved on by using cobalt chromium as a new stent backbone material. Recently, cobalt chromium [13] has been proposed to replace stainless steel [5, 14]. Cobalt chromium stents can be manufactured with thinner struts, improved flexibility, and similar radiopacity and radial strength compared with stainless steel stents [5]. Furthermore, thinner struts have been associated with significant reduction of late in-stent stenosis [2, 14].

Late in-stent stenosis and thrombogenicity were defined as primary study end points. Vessel wall injury and inflammation were evaluated as secondary study end points. For the latter, a semiquantitative immunomicroscopic method was applied.

Methods

Stents and PZF Nanocoat

The stents (16 mm in length; stainless steel 316L or cobalt chromium) were custom made. They had a sinusoidal design and a strut thickness of 110 μm for stainless steel stents and 80 μm for cobalt chromium stents. The unexpanded and uncrimped diameter was 1300 μm. Stent coating process and coating quality control have been previously published in detail [9]. In this study, the average coat thickness was 25 ± 17 nm as determined indirectly by gravimetric measurements. The stents were machine crimped on compliant balloon catheters with a target balloon diameter between 2.5 and 3.5 mm, according to the respective inflation pressure, and a length of 20 mm. The stents underwent ethylene oxide sterilization before packaging.

Coating Integrity

The coating integrity of sterilized PZF-nanocoated stents was tested in two different steps:

Step 1. Two PZF-nanocoated cobalt chromium stents and two PZF-nanocoated stainless steel stents (four stent-balloon catheter assemblies total) were, ex vivo, expanded to the target diameter and evaluated for polymer cracks or other imperfections by scanning electron microscopy (SEM).

2. Two PZF-nanocoated cobalt chromium stents and two PZF-nanocoated stainless steel stents (4 stent-balloon catheter assemblies total) were, ex vivo, pushed through and pulled back twice through the same type of vascular sheath used for the animal experiments. After this, they were expanded to the target diameter and evaluated by SEM.

Animal Preparation and Instrumentation

Thirty female mini-pigs (Goettinger, Ellegaard, Denmark) with a body weight of 25 to 30 kg were equally subdivided with respect to a follow-up interval of either 4 or 12 weeks as well as stent type: (1) bare cobalt chromium stents (BCCS), (2) PZF-nanocoated cobalt chromium stents (PCCS), (3) and PZF-nanocoated stainless steel stents (PSSS), resulting in six subgroups with five animals in each subgroup. The study was conformed to the Guide for the Care and Use of Laboratory Animals [15].

The pigs were sedated with 10 mg azaperon/kg (Stresnil, Janssen-Cilag GmbH, Neuss, Germany) before general anesthesia was introduced with intramuscular injection of 10 mg ketamine/kg (Ketanest S, Essex Pharma GmbH, Munich, Germany) and 1 mg midazolam/kg (Dormicum, Hoffmann-LaRoche AG, Basel, Switzerland). Anesthesia was maintained with titrated intravenous injections of 10 mg ketamine/kg and 1 mg/kg midazolam. The pigs received 1 mg nitroglycerine suspended in 500 ml normal saline and 250 mg acetylsalicylic acid administrated by way of an intravenous line to reduce spasms.

Stenting Protocol

The right femoral artery was surgically exposed and punctured with a regular 3F puncture needle (Bard, Karlsruhe, Germany), and a 5F introduction sheath (Terumo, Tokyo, Japan) was inserted. Subsequently heparin (100 IU/kg) was administered. In our study, we choose the right coronary artery (RCA) as target vessel because of extreme variability of the left coronary artery anatomy (branching, diameter) and to avoid bias from deploying stents in different vessels of the same animal. A 5F Berenstein catheter (Cordis, Miami, FL) was positioned in the proximal RCA to obtain single plain coronary arteriograms (Siemens Polystar Top, field of view 14 cm, 1024×1024 matrix, frame rate 6 images/s; Siemens, Erlangen, Germany). The stent was deployed by an investigator, who was blinded to the type of the stent, by maintaining a balloon inflation pressure of 9 to 13 ATM (depending on the target vessel diameter) for a period of 30 seconds to achieve the desired vessel-to-stent diameter ratio of between 1:1.1 and 1:1.2. Control angiography was performed to confirm successful stent implantation and was

followed by a second bolus injection of 250 mg acetylsalicylic acid. Finally, the arteriotomy was sutured and the wound closed. No additional anticoagulation or antiplatelet medication was administered during follow-up.

Follow-up Procedure and Quantitative Angiography

For the 4- or 12-week periods after the implant procedure process, instrumentation of the pigs and angiographic technique were identical to those during the implantation procedure process except that the left femoral artery was used as the vascular approach. For quantitative angiographic analysis, the following measurements and determinations were performed using the software of the angiographic unit: prestent: the target vessel diameter (TVD) was calculated from five adjacent reference points along the preselected coronary artery and poststent: the average stent diameter (STD) was calculated from three in-stent reference points.

At follow-up angiography, average luminal diameter (ALD) was calculated from 3 in-stent reference points corresponding to the previous STD measurements. Furthermore, the minimal luminal diameter (MLD) was determined from the narrowest angiographic in-stent site at follow-up. Absolute and percentage average late loss were calculated by relating ALD to STD. Absolute and percentage maximum late loss were calculated by relating MLD to STD. For angiographic evaluation of thrombogenicity, a thrombotic event was assumed when a focal filling defect was seen within the stented area or within its immediate adjacent vessel segments.

Tissue Harvest and Microscopic Examination

After the mini-pigs were killed, pressure fixation of the RCA was performed with 4% neutral buffered formalin at 120 mm Hg for a period of 10 minutes using the angiographic catheter in the RCA. The heart was harvested and further immersion-fixed in 4% neutral buffered formalin. The stented coronary artery segments were embedded in hydroxyethylmethacrylate (Technovit 8100, Heraeus Kulzer GmbH, Wehrheim, Germany).

Cross-sectional planes were sawed from the proximal, middle, and distal in-stent sections and from the vessel segment proximal and distal to the stent, and the stent wires were left intact to minimize potential artifacts from removal of the stent wires. The planes were ground and polished to a thickness of approximately 15 μm for staining with toluidine. To determine neointimal thickness, the intimal layer was measured centrally on top of each visible stent strut for each specimen. Presence or absence of thrombus formation within the stented segment or within the adjacent arterial segment was noted. Microscopic analysis was performed by an observer who was blinded to the type of the stent. The vessel wall injury score was determined according to Schwartz [16], and the inflammation score was determined as described by Kornowski [17].

Semiquantitative Immunohistomorphometry

Further sections of every stent were sawed, ground, and polished to a thickness of approximately 8 μm for immunostainings with markers for CRP (1:200 polyclonal pure rabbit antisheep CRP, BioTrend, Cologne, Germany), TNFα (1:200 polyclonal rabbit antimouse TNFα, Genzyme, Neu-Isenburg, Germany), and TGFβ (1:100 polyclonal rabbit antihuman TGFβ1, Santa Cruz Biotechnology, Heidelberg, Germany).

A semiquantitative immunoreactivity score was calculated for each marker and for all vessel wall layers separately (intima, media, adventitia), and this ranging from 0 to 12 as described previously in the pathology context of rheumatology [18]. The definite score was then calculated as the product of the semiquantitative score for the intensity of immunostaining (0 = negative, 1 = poor intensity, 2 = moderate intensity, and 3 = severe intensity) and the semiquantitative score for the percentage of positively stained cells (0 = negative, 1 = <10%, 2 = 10% to 50%, 3 = 51% to 80%, and 4 = >80%). As controls, segments from unstented left coronary arteries were obtained and stained with the same immunomarkers.

Statistical Analysis

Statistical analysis was performed in collaboration with our institutional department of statistics and biometry. All quantitative angiographic and microscopic data were computed in a database. From these, descriptive statistics were calculated. All data were presented as mean ± sd for every single cross-section, stent, and study group, and $p < 0.05$ was regarded as statistically significant. Nonparametric Wilcoxon signed rank test was applied for comparison of all numeric data of BCCS versus PCCS and PCCS versus PSSS for 4- and 12 week follow-up (independent matched pairs) to allow the best possible intergroup discrimination. These statistical procedures were performed with Statview 5.0 (Statistical Analyses System; SAS Institute, Cary, NC).

Results

In Vitro Evaluation of Stent Surfaces

Optical microscopy inspection of the stent surfaces was performed as quality control before sterilization, and

packaging showed smooth and even surfaces on all 20 PZF-coated stents. Contact angle measurements showed a homogeneous coating layer without detectable variations.

Coating Integrity

In none of the two investigational settings was there any polymer disintegration or cracks from ethylene oxide sterilization, mechanical stress resulting from sheath passage, or balloon expansion (Fig. 1).

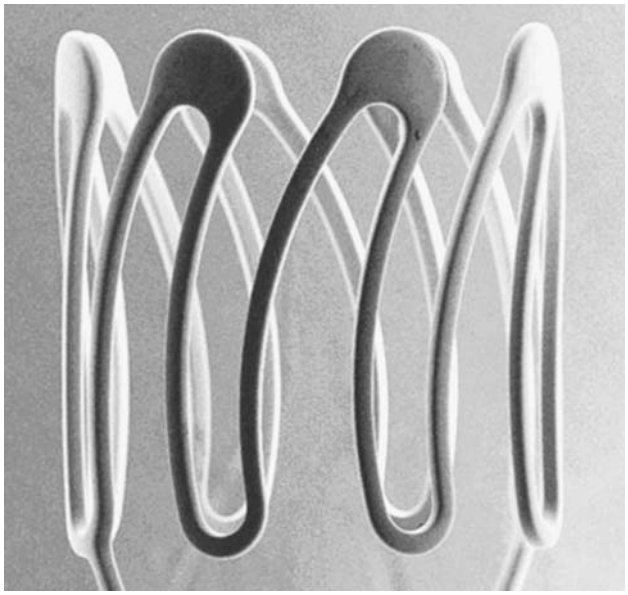

Fig 1 SEM of a PZF-coated cobalt chromium stent after sterilization and balloon expansion. No cracks or damages are detectable

Overall Procedural Success

Thirty stents (10 BCCS, 10 PCCS, and 10 PSSS) were successfully deployed in the RCAs of 30 mini-pigs. A coronary spasm occurred in three pigs with BCCS (one in the 4-week group and two in the 12-week group), in three pigs with PCCS (1 in the 4-week group and two in the 12-week group), and in one pig with PSSS (in the 12-week group). These seven animals received an incremental dose of 250 μg nitro into the RCA using the catheter. In six pigs, the spasms resolved completely within 15 minutes. However, in one pig with PCCS (4-week group), a stenosis 0.5 cm distal to the stent and initially interpreted as spasm persisted throughout the procedure.

Throughout both follow-up intervals, all 30 mini-pigs, including the one pig with the aforementioned in-segment RCA stenosis, presented with good health until they were killed. Later, on both angiography and microscopy, the reason for this persistent stenosis was identified as mural hematoma.

Quantitative Angiography

Angiography performed immediately after stenting did not show on-stent or target vessel thrombus deposition or acute dissection and neither did angiography at killing (Table 1 and Fig. 2).

TVD was similar for both follow-up intervals and stent types (range 2.76 to 2.9 mm). STD after stent deployment was also similar (range 2.89 to 3.08 mm). TVD and STD were not statistically significant between the two follow-up intervals and stent types. The percentage overdilatation ranged between 2.1% and 9.2%, which was also not significantly different. The ALDs of the three stent types had a

Table 1 Quantitative Angiography[a]

	BCCS (range)	PCCS (range)	PSSS (range)
ALD (mm) 4w	2.22 ± 0.42 (1.7–2.7)	2.55 ± 0.68 (1.4–3.0)[b]	2.56 ± 0.27 (2.3–3)
ALD (mm) 12w	2.48 ± 0.23 (2.1–2.7)	2.8 ± 0.25 (2.5–3.2)	2.46 ± 0.43 (1.9–3.1)
MLD (mm) 4w	1.87 ± 0.43 (1.1–2.3)	2.32 ± 0.82 (0.9–2.9[b])	2.24 ± 0.38 (2–2.9)
MLD (mm) 12w	**2.07 ± 0.21[c] (1.8–2.3)**	**2.61 ± 0.24[c] (2.4–3)**	**2.14 ± 0.56[c] (1.4–2.9)**
AL (%) 4w	23.07 ± 12.15 (7.1–33.3)	9.93 ± 16.42 (0–44[b])	11.71 ± 7.14 (0–18.75)
AL (%) 12w	**9.73 ± 4.93[d] (4.5–16.7)**	**2.1 ± 3.05[d] (0–6.7)**	**9.71 ± 7[d] (3.8–17.4)**
MaxL (%) 4w	38.79 ± 11.31 (25.8–56)	19.12 ± 25.63 (2.13–64[b])	22.73 ± 11.81 (3.3–34.4)
MaxL (%) 12w	**24.25 ± 9.8[e] (13.6–40)**	**8.7 ± 2.3[e] (6.25–11.7)**	**22.1 ± 12.6[e] (7.7–39.1)**

[a] Statistically significant results are shown in bold type

[b] Broad value range for PCCS because of in-segment stenosis distal to stent site resulting from wall hematoma in one animal

[c] Statistically significant: BCCS versus PCCS and PCCS versus PSSS ($p = 0.04$)

[d] Statistically significant: BCCS versus PCCS and PCCS versus PSSS ($p = 0.04$)

[e] Statistically significant: BCCS versus PCCS and PCCS versus PSSS ($p = 0.04$)

BCCS = bare cobalt chromium stents; PCCS = PZF nanocoated cobalt chromium stents; PSSS = PZF nanocoated stainless steel stents

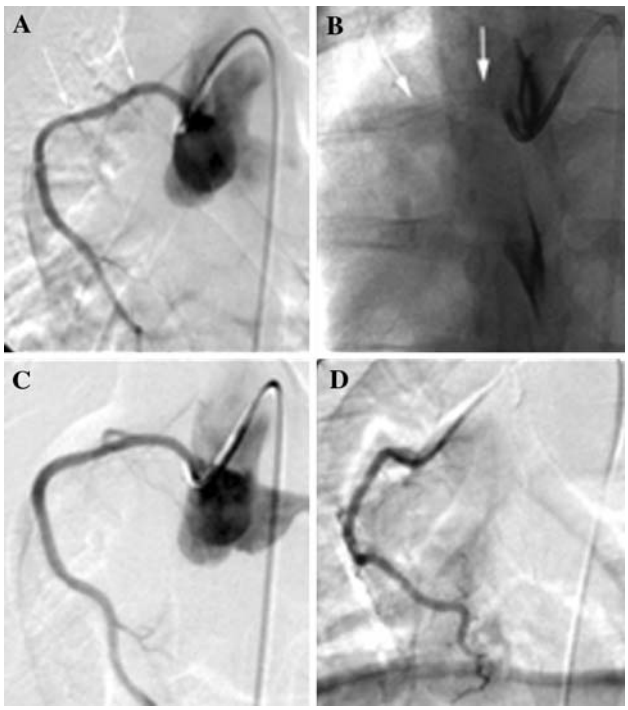

Fig 2 PCCS angiography. (**A**) RCA arteriogram before stent implantation (arrows = target stent implantation site). (**B**) Implanted stent (arrows). (**C**) Arteriogram after stent placement. (**D**) Twelve-week follow-up: no late loss

range of 2.22 to 2.56 mm at 4 weeks and 2.46 to 2.8 mm at 12 weeks follow-up which was without statistically significant difference.

Average MLD at 4 weeks was best in PCCS (2.32 ± 0.82 mm). However, the differences compared with either BCCS (1.87 ± 0.43 mm) or PSSS (2.24 ± 0.38 mm) were not statistically significant. Average MLD at 12 weeks again was best in PCCS (2.61 ± 0.24 mm). The differences compared with either BCCS (2.07 ± 0.21 mm) or PSSS (2.14 ± 0.56 mm) were statistically significant ($p = 0.04$).

The AL of 0.2 ± 0.49 mm and the %AL of 9.93% ± 18.62% of PCCS at 4 weeks was best compared with the other two stent types at 4 weeks; however, this was without statistical significance. At 12 weeks the best result was again found in PCCS, with an AL of 0.06 ± 0.09 mm and an %AL of 2.1% ± 3.05%. The differences compared with the two other stent types were statistically significant ($p = 0.04$).

Accordingly, at 12 weeks the maximum loss (MaxL) in PCCS determined in mm (0.25 ± 0.07 mm) and in % (8.75% ± 2.32%) was significantly lower compared with the two other stent types ($p = 0.04$). However, no significant differences were detected at 4 weeks between the three stent types. The mini-pig with the mural hematoma (PCCS at 4 weeks) had the worst individual angiographic appearance as demonstrated in detail in Table 1.

Microscopy

The average neointimal thickness in BCCS was 136 ± 144.2 μm after 4 weeks and 74.7 ± 57.6 μm after 12 weeks. The average PCCS neointimal thickness was 152 ± 273.7 μm at 4 weeks and 40.7 ± 16 μm at 12 weeks. PSSS showed an average neointimal thickness of 111.3 ± 14.6 μm after 4 weeks and of 141.5 ± 109 μm after 12 weeks. This low neointimal thickness of PCCS after 12 weeks reached the level of statistical significance compared with BCCS and PSSS ($p = 0.04$) (Table 2 and Fig. 3).

The %stenosis of BCCS was 41.5% ± 12.4% after 4 weeks and 33.9% ± 4.2% after 12 weeks. In PCCS, it was 35.8% ± 24.8% after 4 weeks and 29.2% ± 6.6% after 12 weeks. In PSSS, the %stenosis was 35.7% ± 2.6% at 4 weeks and 40.3% ± 13.9% at 12 weeks. The differences never reached statistical significance.

Interestingly, the one animal with the post-stent wall hematoma (see previous text) had the worst microscopic

Table 2 Microscopy[a]

	BCCS (range)	PCCS (range)	PSSS (range)
Neointima (μm) 4w	136 ± 144.2 (33.4–377.4) 222 struts	152 ± 273.7 (5–638.4)[b] 236 struts	111.3 ± 14.5 (95.6–127.2) 218 struts
Neointima (μm) 12w	**74.7 ± 57.6[c] (38.6–175.2) 216 struts**	**40.7 ± 15.9[c] (20.8–65) 226 struts**	**141.5 ± 109[c] (27–295.2) 231 struts**
%Stenosis, 4w	41.5 ± 12.4 (31.2–62.4)	35.8 ± 24.8 (17–79)	35.7 ± 2.6 (32–38.5)
%Stenosis, 12w	33.9 ± 4.2 (29.6–40.1)	29.2 ± 6.6 (23–39.5)	40.2 ± 13.9 (22.7–55.9)
Injury score 4w	1.1 ± 0.13	1.19 ± 0.14	1.1 ± 0.07
Injury score 12w	0.98 ± 0.05	1.04 ± 0.06	1.09 ± 0.12
Inflammation score 4w	0.2 ± 0.1	0.3 ± 0.2	0.2 ± 0.1
Inflammation score 12w	0.1 ± 0.1	0.1 ± 0.1	0.3 ± 0.4

[a] Statistically significant results are shown in bold type

[b] Extreme range value for PCCS at 4 weeks because of in-segment stenosis distal to stent site resulting from wall hematoma in one animal

[c] Statistically significant: $p = 0.04$

BCCS = bare cobalt chromium stents; PCCS = PZF nanocoated cobalt chromium stents; PSSS = PZF nanocoated stainless steel stents

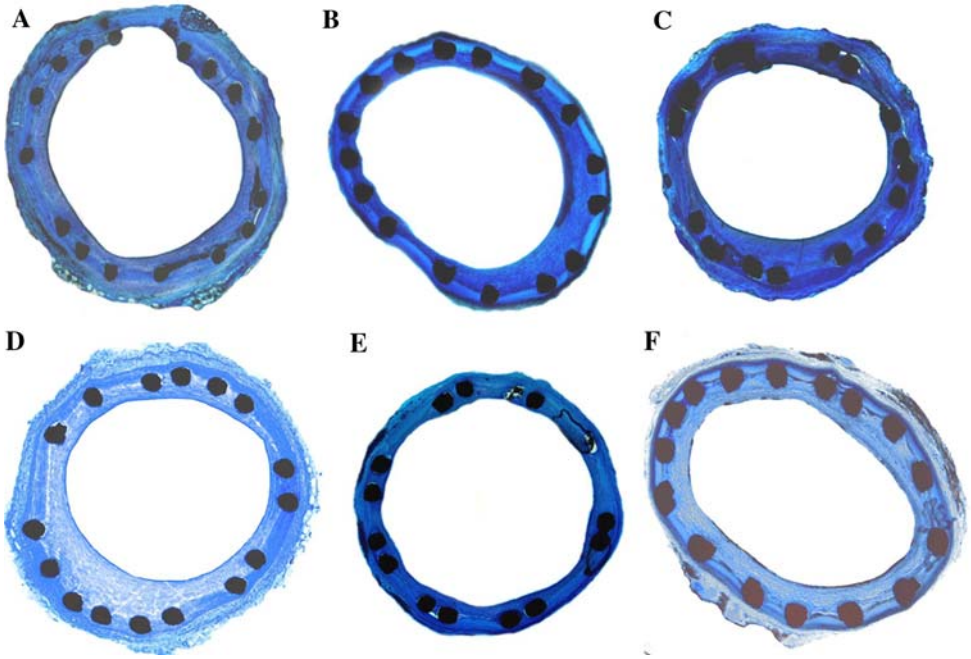

Fig 3 Cross-section micrographs at 4 and 12 weeks (4× original magnification, toluidin blue staining). (**A**) BCCS at 4 weeks: neointima ranging from 0 to 140 µm. (**B**) PCCS at 4 weeks: neointima ranging from 5 to 145 µm. (**C**) PSSS at 4 weeks: neointima ranging from 0 to 145 µm. (**D**) BCCS at 12 weeks: neointima ranging from 10 to 160 µm. (**E**) PCCS at 12 weeks: neointima ranging from 5 to 35 µm. (**F**) PSSS at 12 weeks: neointima ranging from 30 to 110 µm

result and dominated the averages for the 4-week PCCS group in neointimal thickness. Macroscopic or microscopic evidence of on-stent thrombus deposition was never observed in any stent group. The injury severity score according to Schwartz ranged between 0.98 and 1.19 and showed no statistically significant differences in any study group.

The inflammation score according to Kornowski was 0.2 ± 0.1 at 4 weeks and 0.1 ± 0.1 at 12 weeks in BCCS and 0.3 ± 0.2 at 4 weeks and 0.1 ± 0.1 at 12 weeks in PCCS. The PSSS showed an inflammation score of 0.2 ± 0.1 after 4 weeks and 0.3 ± 0.4 after 12 weeks. Severe inflammatory reactions with granulomata were not observed in any stent group. The results of the inflammation scores showed no statistically significant differences in any follow-up group.

Semiquantitative Immunohistomorphometry

CRP immunomicroscopy showed minimal or low-grade inflammation (2.2 to 5.2) in all stent groups and vessel wall layers, which was without statistical significance. In TNFα immunomicroscopy, minimal or low-grade inflammation (1 to 1.8) was detected in all stent groups and vessel wall layers, and this was without statistical significance. TGFβ immunomicroscopy showed minimal or low-grade inflammation (1 to 3.6), and this was without statistically significant difference between the study groups and vessel wall layers (Fig. 4). Immunopositive cells close to stent struts were observed in all immunostainined macrophages. The controls from unstented left coronary artery segments showed no immunomarker expression.

Discussion

The purpose of this study was twofold: (1) to investigate whether PZF coating of a cobalt chromium stent with thinner struts might furthermore decrease the already very favourable results of stainless steel stents and (2) how the coating influences angiographic and microscopic patterns of neointima formation and late in-stent stenosis. Overall, all stents performed well, with overall low late loss; however, the combination of a cobalt chromium metal backbone and PZF nanocoat showed the significantly best results at long-term follow-up in direct comparison of the three groups. Several explanations are conceivable for the favourable performance of this combination.

To maintain visibility during delivery and reliable expansion ratios, stainless steel stents must have relatively thick struts (>100 µm) for coronary artery stent designs. Increasing strut thickness can result in greater vessel wall injury, inflammation, and in-stent stenosis [2]. Backbone materials allowing thinner stent struts have been intensively investigated and, in this context, cobalt chromium is becoming a more frequently used metal. It provides, along with remarkably thinner struts, the same radiopacity, the same radial strength, greater flexibility, and easier deliverability than stainless steel [5, 14]. The injury scores in our study were similar, ranging between 0.98 and 1.19, which is without statistically significant difference, and showing good stent adaptation to the vessel wall without major damage in both cobalt chromium and stainless steel stents. Consequently, this study showed no effect of strut thickness on vessel wall injury compared with the results of previous studies [2]. Whereas these studies used stents with

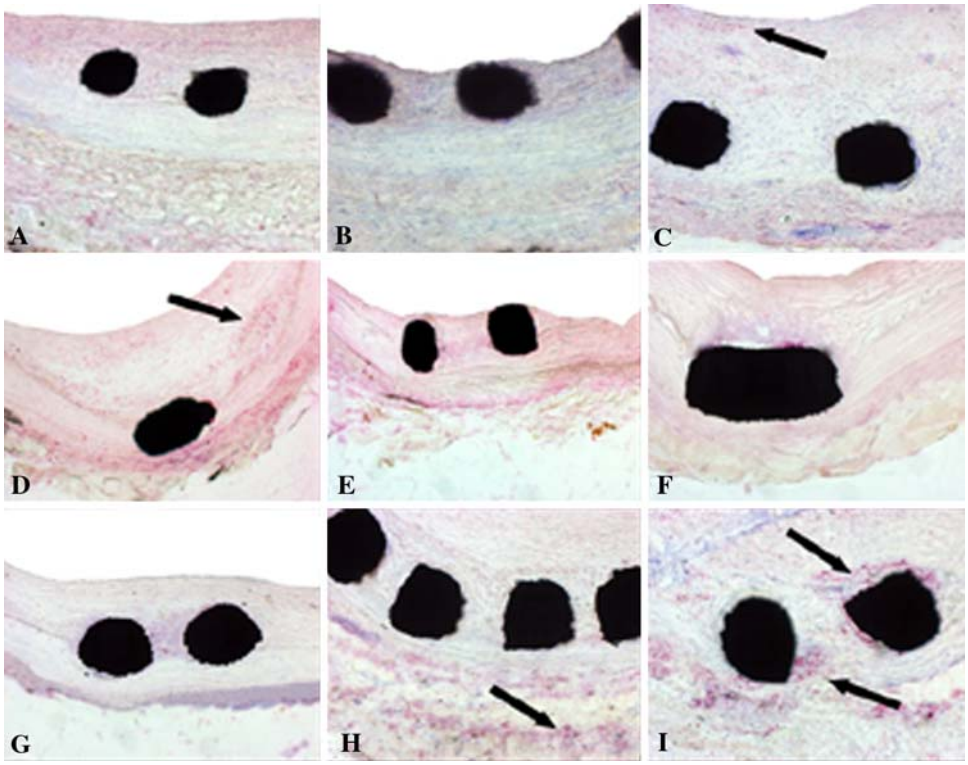

Fig 4 Cross-section micrographs of immunomicroscopy at 12 weeks (30× original magnification). (**A**) BCCS: CRP immunostaining. (**B**) PCCS: CRP immunostaining. (**C**) PSSS: CRP immunostaining. (**D**) BCCS: TNFα immunostaining. (**E**) PCCS: TNFα immunostaining. (**F**) PSSS: TNFα immunostaining. (**G**) BCCS: TGFβ immunostaining. (**H**) PCCS: TGFβ immunostaining. (**I**) PSSS: TGFβ immunostaining. Black arrows show immunomarker expression

50- and 140-μm strut thickness with an absolute difference of 90 μm, our study design provided BCCS and PCCS with a strut thickness of 80 μm and PSSS with a strut thickness of 110 μm. The similarity of the injury scores in "thin" and "thick" strut stents could be explained (1) by the moderate strut thickness difference (30 μm) and (2) by the absolute strut thickness, with a maximum of 110 μm, even in PSSS. It has been reported that endothelial cell coverage decreases in stent struts thicker than 75 μm and, conversely, is facilitated in stents with thinner struts [19]. This might explain the favourable performance of thin-strut cobalt chromium stents because complete endothelial cell growth is an important factor in preventing neointimal hyperplasia [20]. It might also explain the trend toward thinner neointimal coverage from 4 to 12 weeks of both coated and uncoated cobalt chromium stents both angiographically and microscopically.

In the study described here, we did not evaluate uncoated stainless steel stents. However, in a porcine coronary artery model of our group, implantation of uncoated stainless steel stents resulted in a neointimal height of 299 μm after 12 weeks [12], and in a rabbit iliac artery study, the neointimal height measured 115 μm in uncoated stainless steel stents [9]. Compared with this, uncoated cobalt chromium stents had an average neointima of only 74.7 μm at the same follow-up interval in our current study.

After stent implantation, the biocompatibility of stent and polymer coating is important because vessel wall inflammation is a potent stimulus for neointimal growth [17]. Previous studies showed controversial results when the effects of different stent polymer coatings on inflammation were evaluated. De Scheerder proved massive tissue reaction, such as vessel wall inflammation and in-stent stenosis upto 81%, in stents covered with biodegradable polyorganophosphazenes [6], whereas Huang and Richter established good biocompatibility and reduced in-stent stenosis using poly(bis(trifluoroethoxy)phosphazene as stent coating [9, 10]. However, in both aforementioned studies, earlier versions of poly-bis(trifluoroethoxy)phosphazene (PTFEP) were used. The polymeric material PZF (Polyzene-F) used for this study has been further improved with respect to molecular weight, purity, and, hence, resistance to degredation by applying proprietory refinement technology. Recently, Radeleff et al [21] showed a low inflammatory reaction in cobalt chromium stents with a Polyzene-F coat thickness of 200 to 400 nm. Also, favourable results with low inflammatory reactions have been reported when PZF was used as a coating for embolic agents [22].

Ranging from 0.1 to 0.3 on average, the inflammation score was low in all groups in our study, suggesting good biocompatibility of PZF, and it even surpassed the results of a previous coronary artery study by our group

(inflammation score of 0.84 in PZF-coated stents after 4 weeks) [12].

Thrombogenicity also plays a key role in the development of restenosis. The acute response after stent implantation includes aggregation of platelets and fibrin at the site of injury, which release attractants for smooth muscle cells, leading to neointimal proliferation [23, 24]. The polyphosphazene/PZF surface adsorbs coagulation-inhibiting proteins, such as human serum albumin and human immunoglobin, instead of coagulation-stimulating proteins, such as fibrinogen, fibronectin, and von Willebrandt factor [7]. In vitro studies showed that platelet adhesion to polyphosphazene was significantly less than in other polymers [25]. These findings were validated by in vivo studies showing thromboresistance of the polyphosphazene nanocoat [9, 10, 12]. In a rabbit iliac artery model, no fibrin or thrombus deposition was found on PTFEP-coated stent surfaces, which were covered by a thin proteinaceous layer, at 1 week, whereas fibrin deposition was evident on bare controls [9]. These "microthrombus" depositions might be one of the (most pertinent) explanations for higher neointima and greater late loss in uncoated stents compared with the PZF-nanocoated stents. In this study, there was no angiographic evidence of "macro"-thrombus deposition, which might also indirectly reflect the low thrombogenicity of PZF.

Study Limitations

Animal models for the study of vessel wall reaction on coronary artery stenting sharpen our picture of in-stent stenosis formation. However, there are some limitations in adapting our results to humans. First, our study design provided stent implantation in nonatherosclerotic coronary arteries of young pigs, although every day human stenting takes place in atherosclerotic coronary arteries of older people. Attempts to create atherosclerosis-like conditions in pigs (with hypercholesterolic diets or by balloon injury) are not adequate to represent the complex atherosclerotic lesions in humans. Therefore, we chose a native porcine coronary artery model similar to that suggested in a consensus article published by Schwartz [26]. Second, the majority of human coronary stenting is carried out in the left coronary artery. Another limitation of our study is the rather small number of animals per group (five) and having only two follow-up intervals (4 and 12 weeks).

In conclusion, a polymer with good biocompatibility including antithrombotic characteristics, potential for endothelial cell coverage, reduction of vessel wall inflammation, and neointimal overgrowth could further enhance the biologic behavior of thin-strut stents. In our study, PZF in combination with a cobalt chromium stent provided favourable results with respect to late loss, thrombogenicity, and vessel wall inflammation and might be an interesting polymer for passive or active stents.

Acknowledgments This study was sponsored in part by CeloNova BioSciences, Newnan, GA. Stampfl, R. Lopez-Benitez, and G. M. Richter have sponsored research agreements with CeloNova BioSciences. G. M. Richter has served as consultant to CeloNova BioSciences.

References

1. Virmani R, Farb A (1999) Pathology of in-stent restenosis. Curr Opin Lipidol 10:499–506
2. Kastrati A, Mehilli J, Dirschinger J et al (2001) Intracoronary stenting and angiographic results: strut thickness effect on restenosis outcome (ISAR-STEREO) trial. Circulation 103:2816–2821
3. Garasic JM, Edelman ER, Squire JC et al (2000) Stent and artery geometry determine intimal thickening independent of arterial injury. Circulation 101:812–818
4. Moses JW, Leon MB, Popma JJ et al (2003) Sirolimus-eluting stents versus standard stents in patients with stenosis in a native coronary artery. N Engl J Med 349:1315–1323
5. Sketch MH Jr, Ball M, Rutherford B et al (2005) Evaluation of the Medtronic (Driver) cobalt-chromium alloy coronary stent system. Am J Cardiol 95:8–12
6. De Scheerder IK, Wilczek KL, Verbeken EV et al (1995) Biocompatibility of polymer-coated oversized metallic stents implanted in normal procine coronary arteries. Atheriosclerosis 114:105–114
7. Welle A, Grunze M, Tur D (2000) Blood compatibility of poly[bis(trifluoroethoxy)phosphazene]. J Appl Med Polym 4:6–10
8. Babapulle MN, Eisenberg MJ (2002) Coated stents for the prevention of restenosis: part II. Circulation 106:2859–2866
9. Richter GM, Stampfl U, Stampfl S et al (2005) A new polymer concept for coating of vascular stents using PTFEP (poly(bis(trifluoroethoxy)phosphazene) to reduce thrombogenicity and late in-stent stenosis. Invest Radiol 40:210–218
10. Huang Y, Liu X, Wang L et al (2003) Long-term biocompatibility evaluation of a novel polymer-coated stent in a porcine coronary stent model. Coron Artery Dis 14:401–408
11. Henn C, Satzl S, Christoph P et al (2008) Efficacy of a polyphosphazene nanocoat in reducing thrombogenicity, in-stent stenosis, and inflammatory response in porcine renal and iliac artery stents. J Vasc Interv Radiol 19:427–437
12. Satzl S, Henn C, Christoph P et al (2007) The efficacy of nanoscale poly[bis(trifluoroethoxy) phosphazene] (PTFEP) coatings in reducing thrombogenicity and late in-stent stenosis in a porcine coronary artery model. Invest Radiol 42:303–311
13. Fischman DL, Leon MB, Baim DS et al (1994) A randomized comparison of coronary-stent placement and balloon angioplasty in the treatment of coronary artery disease. Stent Restenosis Study Investigators. N Engl J Med 331:496–501
14. Kereiakes DJ, Cox DA, Hermiller JB et al (2003) Usefulness of a cobalt chromium coronary stent alloy. Am J Cardiol 92:463–466
15. Bayne K (1996) Revised guide for the care and use of laboratory animals available. American Physiological Society. Physiologist 39(199):208–211
16. Schwartz RS, Huber KC, Murphy JG et al (1992) Restenosis and the proportional neointimal response to coronary artery injury: results in a porcine model. J Am Coll Cardiol 19:267–274
17. Kornowski R, Hong MK, Tio FO et al (1998) In-stent restenosis: contributions of inflammatory responses and arterial injury to neointimal hyperplasia. J Am Coll Cardiol 31:224–230

18. Finis K, Sultmann H, Ruschhaupt M et al (2006) Analysis of pigmented villonodular synovitis with genome-wide complementary DNA microarray and tissue array technology reveals insight into potential novel therapeutic approaches. Arthritis Rheum 54:1009–1019
19. Simon C, Palmaz JC, Sprague EA (2000) Influence of topography on endothelialization of stents: clues for new designs. J Long Term Eff Med Implants 10:143–151
20. Schatz RA (1989) A view of vascular stents. Circulation 79:445–457
21. Radeleff B, Thierjung H, Stampfl U et al (2007) Restenosis of the CYPHER-Select, TAXUS-Express, and Polyzene-F Nanocoated Cobalt-Chromium Stents in the minipig coronary artery model. Cardiovasc Intervent Radiol (Epub ahead of print)
22. Stampfl S, Stampfl U, Bellemann N et al (2008) Biocompatibility and recanalization characteristics of hydrogel microspheres with polyzene-f as polymer coating. Cardiovasc Intervent Radiol (Epub ahead of print)
23. Schwartz RS, Chronos NA, Virmani R (2004) Preclinical restenosis models and drug-eluting stents: still important, still much to learn. J Am Coll Cardiol 44:1373–1385
24. Schwartz RS, Holmes DR Jr, Topol EJ (1992) The restenosis paradigm revisited: an alternative proposal for cellular mechanisms. J Am Coll Cardiol 20:1284–1293
25. Tur DR, Korshak VV, Vinogradova SV et al (1986) Effects of biological medium on the properties of poly[bis(trifluoroethoxy)phosphazene]. Acta Polym 37:203–208
26. Schwartz RS, Edelman ER, Carter A et al (2002) Drug-eluting stents in preclinical studies: recommended evaluation from a consensus group. Circulation 106:1867–1873